ISSN/2499-5347

E. NICHELATTI

Nuclear Department
Physical Technologies and Safety Division
Particle Accelerator Laboratory
Casaccia Research Centre, Rome - Italy

ENERGY SPECTRUM AND BRAGG CURVE OF A PROTON BEAM IN LOW-DENSITY LITHIUM FLUORIDE

RT/2025/14/ENEA

ITALIAN NATIONAL AGENCY FOR NEW TECHNOLOGIES,
ENERGY AND SUSTAINABLE ECONOMIC DEVELOPMENT

E. NICHELATTI

Nuclear Department
Physical Technologies and Safety Division
Particle Accelerator Laboratory
Casaccia Research Centre, Rome - Italy

ENERGY SPECTRUM AND BRAGG CURVE OF A PROTON BEAM IN LOW-DENSITY LITHIUM FLUORIDE

RT/2025/14/ENEA

ITALIAN NATIONAL AGENCY FOR NEW TECHNOLOGIES,
ENERGY AND SUSTAINABLE ECONOMIC DEVELOPMENT

ENERGY SPECTRUM AND BRAGG CURVE OF A PROTON BEAM IN LOW-DENSITY LITHIUM FLUORIDE

E. Nichelatti

Abstract
Irradiation of lithium fluoride (LiF) with a proton beam induces the formation of F2 and F3+ aggregate color centers that luminesce in the visible spectrum when optically excited by blue light. The spatial distribution of the emitted radiophotoluminescence is proportional to the proton Bragg curve in LiF, provided that the dose received by the material is not too high (less than approximately 105–106 Gy) to cause saturation of the center density. From the analysis of the luminescent Bragg curve, it is possible to estimate the energy spectrum of the proton beam. If the analysis method is based on the superposition of theoretical Bragg curves calculated in bulk LiF, but the irradiated LiF is a thin film with a packing density lower than 100%, the resulting spectrum will not reflect the actual one. In fact, protons in a material with lower density than bulk penetrate deeper than they would in bulk. In this Technical Report, I derive an approximate correction formula that allows obtaining the actual spectrum in lower-density LiF.

Keywords: *proton beam, energy spectrum, Bragg curve, lithium fluoride, color centers, radiophotoluminescence.*

Sommario
L'irraggiamento del fluoruro di litio (LiF) con un fascio di protoni provoca la formazione di centri di colore aggregati F2 ed F3+ che emettono luminescenza nel visibile se eccitati otticamente con luce blu. La distribuzione spaziale della radiofotoluminescenza emessa è proporzionale alla curva di Bragg dei protoni nel LiF, purché la dose ricevuta dal materiale non sia troppo elevata (minore di circa 105–106 Gy) da provocare saturazione della densità dei centri. Dall'analisi della curva di Bragg luminescente, è possibile stimare lo spettro energetico del fascio di protoni. Se il metodo di analisi si basa sulla sovrapposizione di curve di Bragg teoriche calcolate nel LiF bulk, ma il LiF irraggiato è quello di un film sottile con densità d'impacchettamento minore del 100%, lo spettro che si ottiene non è quello reale. Infatti, i protoni in un materiale con densità inferiore a quella di bulk penetrano più in profondità rispetto a quanto farebbero nel bulk. In questo Rapporto Tecnico, derivo una formula correttiva approssimata che permette di ricavare lo spettro reale nel LiF a densità minore.

Parole chiave: fascio di protoni, spettro energetico, curva di Bragg, fluoruro di litio, centri di colore, radiofotoluminescenza.

INDEX

1. Introduction

The visualization and subsequent processing of radiophotoluminescent Bragg curves, generated in the visible spectrum by spatial distributions of stable aggregate F_2 and F_3^+ color centers in lithium fluoride (LiF) – formed through proton energy deposition in the material and consisting of two electrons bound to two and three anion vacancies, respectively – has become a well-established method for characterizing the energy spectrum of proton beams in the range from just under 1 MeV to several tens of MeV [1–6]. For low energies (typically below 10 MeV), an approach based on random optimization – also known as localized random search [7] – uses a look-up-table (LUT) of simulated Bragg curves in bulk LiF (density $\rho_0 = 2.635$ g/cm^3 [8]), generated with the Monte Carlo (MC) software FLUKA [9–12]. This method enables the estimation of the proton energy spectrum by performing a best fit of the radiophotoluminescent Bragg curve imprinted in LiF [5].

When the material irradiated by the proton beam – assumed to be laterally extended and collimated – is a LiF crystal, and the irradiation geometry involves grazing incidence to enable proper recording of the Bragg curve, specific models have been developed to account for fluence losses due to multiple Coulomb scattering [4] and for the effects of small angular misalignments between the beam and the crystal [6].

When dealing with a thin LiF film irradiated at grazing incidence by the proton beam, it is important to note that proton migration from the substrate on which the film is deposited can distort the Bragg curve imprinted in the film compared to that observed in a LiF crystal. This effect becomes particularly significant for proton energies above approximately 2 MeV in the case of 1–2 μm thick films deposited on 0.5 mm thick silicon substrates (Si(100) faces) [13]. In addition to this, another key factor must be considered: the density ρ of a LiF film is typically lower than that of bulk LiF (ρ_0). This reduced density leads to deeper proton penetration and a corresponding modification of the Bragg curve within the material.

In this Technical Report, known empirical laws are employed to derive the modifications to the Bragg curve caused by reduced material density, and to assess how these changes affect the estimation of the proton energy spectrum obtained through Bragg curve analysis.

2. Theory

Consider a proton beam irradiating at grazing incidence a thin LiF film deposited on a substrate. The energy deposited by the protons in the material generates a spatial density distribution of aggregate F_2 and F_3^+ color centers, which are photoluminescent in the visible range at room temperature. This distribution is proportional to the Bragg curve in LiF – provided that the proton energy is not high enough to cause significant migration of beam protons scattered from the substrate into the film, thereby distorting the Bragg curve [13]. Furthermore, if the LiF film has a material density ρ lower than the bulk density ρ_0, due to a packing density below 100%, the resulting Bragg curve extends deeper into the material. This effect manifests as a kind of stretching which – as will be shown – depends on the ratio ρ/ρ_0.

Using the Bragg-Kleeman laws and the definition of stopping power, an approximate relationship can be derived between the Bragg curve in low-density LiF and the standard Bragg curve in bulk LiF. Building on this result, an approximate relationship is then deduced between the fictitious energy spectrum – obtained by analyzing the photoluminescent Bragg curve in low-density LiF under the assumption of bulk density ρ_0 – and the actual spectrum that would be obtained by correctly accounting for the reduced density ρ. This correction is particularly relevant when using a recently published

method for energy spectrum estimation that relies on a LUT of Bragg curve simulations in bulk LiF [5] and does not incorporate the possibility of reduced material density.

2.1 Proton range and kinetic energy

In a material, the range R_0 of monochromatic protons with kinetic energy E_0 is governed by the empirical Bragg-Kleeman law (which is an approximation compared to more rigorous formulations),

$$R_0 = \alpha E_0^p, \tag{1}$$

where α and p are two characteristic parameters of the material. This law loses validity at energies below a few hundred keV, where nuclear interactions between protons and the nuclei of the material become more significant than Coulomb interactions with the electrons. Through MC simulations using the SRIM software [14,15] and allometric fitting of the results, it has been verified that, in the energy range between 0.5 and 7 MeV, the parameters for LiF are approximately $p \approx 1.71$ and $\alpha \approx 11.2$ μm/MeV^p. These MC simulations were performed assuming the standard bulk density for LiF, $\rho_0 = 2.635$ g/cm^3 [8].

If the material has a density ρ lower than that of bulk – such as in the case of a thin polycrystalline film where voids exist between grains – the range of protons in the material increases. In fact, another empirical formula, also referred to as the Bragg-Kleeman law, relates the ranges R_1 and R_2 of protons with the same initial kinetic energy in two different materials through the expression [16]

$$\frac{R_1}{R_2} = \frac{\rho_2}{\rho_1}\sqrt{\frac{A_1}{A_2}}, \tag{2}$$

where ρ_1 and ρ_2 are the densities, and A_1 and A_2 are the effective mass numbers of the two materials. This formula can also be applied to the special case of materials with identical composition but different densities – such as low-density LiF compared to bulk LiF. In this case, the range $R_{0,\rho}$ in low-density LiF is related to the range R_0 in bulk LiF by [17]

$$R_{0,\rho} = \frac{\rho_0}{\rho} R_0 = \frac{\rho_0}{\rho} \alpha E_0^p = \alpha_\rho E_0^p \, . \tag{3}$$

Practically, the decrease in density can be expressed as a modification $\alpha \to \alpha_\rho \equiv (\rho_0/\rho)\alpha$, in order to preserve the functional form of the Bragg-Kleeman law under reduced-density conditions.

It should be noted, however, that the previous formula can also be expressed as

$$R_{0,\rho} = \alpha E_{0,\rho}^p \, , \tag{4}$$

where $E_{0,\rho}$ is a fictitious energy defined as

$$E_{0,\rho} \equiv \left(\frac{\rho_0}{\rho}\right)^{1/p} E_0 \, . \tag{5}$$

Maintaining the same value of α as in bulk LiF in Eq. (4) effectively corresponds to assuming that proton propagation occurs in a material with unchanged density ρ_0, while the initial energy of the protons is modified. In other words, this can be interpreted as an equivalence – regarding the range – between the

propagation of protons with initial energy E_0 in LiF of density ρ, and the propagation of protons with initial energy $E_{0,\rho}$ in LiF of density ρ_0. As shown below, this equivalence can be exploited to establish a relationship that enables the deduction of the actual energy spectrum of protons in low-density LiF after estimating it under the assumption that the material had bulk density.

2.2 Stopping power and Bragg curve

Suppose we have an estimate of the energy spectrum of a proton beam that irradiated a LiF film with density $\rho < \rho_0$ at grazing incidence, but the estimate was obtained under the assumption that the LiF material had density ρ_0. This situation can occur, for example, when using a best-fit algorithm to deduce the energy spectrum from the luminescent Bragg curve imprinted in LiF, if the algorithm relies on a LUT of Bragg curves simulated in bulk LiF using MC software – as is the case of the adaptive random optimization (ARO) algorithm for low energies (below 10 MeV), introduced in [5].

In the case of a thin film with a density lower than that of the bulk material, the energy spectrum can, in principle, be estimated using the ARO algorithm, provided that the proton energy does not exceed a threshold beyond which the migration of scattered protons from the underlying substrate significantly alters the Bragg curve imprinted in the film [13]. However, since the ARO algorithm employs a LUT of Bragg curve simulations in bulk LiF, i.e., with density ρ_0, the spectrum obtained must be corrected to account for the lower density of the film. This correction can be applied using the following approach.

To calculate the energy variation of protons in bulk LiF along the mean propagation axis z, Eq. (1) is applied to the relationship between the remaining distance, $R_0 - z$, to reach the range and the energy at that point, E(z), obtaining [18]

$$E(z) = \left(\frac{R_0 - z}{\alpha}\right)^{1/p} = \left(E_0^p - \frac{z}{\alpha}\right)^{1/p}. \tag{6}$$

From this formula, the stopping power, $S(E_0, z)$, is derived. This quantity gives rise to the Bragg curve through the subsequent insertion of fluence and integration over the statistical distribution of proton stopping positions. The stopping power is given by [19]

$$S(E_0, z) = -\frac{dE}{dz}(z) = \frac{1}{\alpha p}\left(E_0^p - \frac{z}{\alpha}\right)^{\frac{1}{p}-1}. \tag{7}$$

If propagation occurs in low-density LiF instead of in bulk material, the previous reasoning can be repeated starting from Eq. (3). In this case, one obtains

$$E_\rho(z) = \left(\frac{R_{0,\rho} - z}{\alpha_\rho}\right)^{1/p} = \left(E_0^p - \frac{z}{\alpha_\rho}\right)^{1/p}. \tag{8}$$

Therefore, the stopping power $S_\rho(E_0, z)$ in low-density LiF is

$$S_\rho(E_0, z) = -\frac{dE_\rho}{dz}(z) = \frac{1}{\alpha_\rho p}\left(E_0^p - \frac{z}{\alpha_\rho}\right)^{\frac{1}{p}-1} = \frac{\rho}{\rho_0}\frac{1}{\alpha p}\left(E_0^p - \frac{\rho}{\rho_0}\frac{z}{\alpha}\right)^{\frac{1}{p}-1}. \tag{9}$$

By comparing Eqs. (7) and (9), one verifies that

$$S_\rho(E_0, z) = \frac{\rho}{\rho_0} S\left(E_0, \frac{\rho}{\rho_0} z\right). \tag{10}$$

The meaning of this equality is as follows: from a mathematical standpoint, the stopping power in low-density LiF is a scaled version of the bulk stopping power. Specifically, it is reduced in intensity by a factor ρ/ρ_0 and stretched in depth by a factor ρ_0/ρ.

An important observation is that Eq. (9) can also be rewritten in the form

$$S_\rho(E_0, z) = \left(\frac{\rho}{\rho_0}\right)^{1/p} \frac{1}{\alpha p} \left(E_{0,\rho}^p - \frac{z}{\alpha}\right)^{\frac{1}{p}-1}, \tag{11}$$

where $E_{0,\rho}$ is the fictitious energy introduced in Eq. (5). This leads to an alternative expression

$$S_\rho(E_0, z) = \left(\frac{\rho}{\rho_0}\right)^{1/p} S\left(E_{0,\rho}, z\right). \tag{12}$$

The meaning of this equality is as follows: the stopping power in low-density LiF is a version of the bulk stopping power, scaled in intensity by a factor $(\rho/\rho_0)^{1/p}$, and evaluated at the fictitious energy $E_{0,\rho} > E_0$.

Assuming that the density difference is sufficiently small, we can reasonably expect that the processing applied to the stopping power to obtain the Bragg curve [18] approximately preserves a relationship similar to Eq. (12) between the Bragg curve in low-density LiF – denoted as $L_\rho(E_0, z)$ – and that in bulk LiF at the fictitious energy $E_{0,\rho}$ – denoted as $L(E_{0,\rho}, z)$. Therefore, we can write

$$L_\rho(E_0, z) = \left(\frac{\rho}{\rho_0}\right)^{1/p} L\left(E_{0,\rho}, z\right). \tag{13}$$

This implies that the Bragg curve in low-density LiF is a scaled version of the bulk Bragg curve evaluated at the fictious energy $E_{0,\rho} > E_0$, with the scaling factor $(\rho/\rho_0)^{1/p}$ applied to its intensity.

2.3 Energy spectrum

If the proton beam is not monochromatic, it is characterized by an energy spectrum whose spectral density is denoted by $\phi(E)$. The corresponding polychromatic Bragg curve in low-density LiF, denoted as $\Lambda_\rho(z)$, can be expressed as a continuous superposition of monochromatic curves weighted by $\phi(E)$ dE, i.e.

$$\Lambda_\rho(z) = \int_0^\infty \phi(E)\, L_\rho(E, z)\, dE\,. \tag{14}$$

By exploiting Eq. (13), this expression can be rewritten in terms of the equivalent Bragg curves in bulk LiF,

$$\Lambda_\rho(z) = \left(\frac{\rho}{\rho_0}\right)^{1/p} \int_0^\infty \phi(E)\, L\left[\left(\frac{\rho_0}{\rho}\right)^{1/p} E, z\right] dE\,. \tag{15}$$

Applying the variable substitution $E' = (\rho_0/\rho)^{1/p} E$, the integral becomes

$$\Lambda_\rho(z) = \left(\frac{\rho}{\rho_0}\right)^{2/p} \int_0^\infty \phi\left[\left(\frac{\rho}{\rho_0}\right)^{1/p} E'\right] L(E', z)\, dE' \,. \tag{16}$$

Let us analyze Eq. (16). It shows that, when best fitting a polychromatic Bragg curve recorded in a film of density ρ, using as a basis the monochromatic curves L(E′, z) corresponding to the bulk density ρ_0, a fictitious energy spectrum is obtained, given by

$$\phi^*(E') = \left(\frac{\rho}{\rho_0}\right)^{2/p} \phi\left[\left(\frac{\rho}{\rho_0}\right)^{1/p} E'\right] \tag{17}$$

The real spectrum can be derived from the fictitious one by applying the substitution $E = (\rho/\rho_0)^{1/p} E'$ to the product $\phi^*(E')\, dE'$. This yields

$$\phi^*(E')\, dE' = \left(\frac{\rho}{\rho_0}\right)^{1/p} \phi(E)\, dE \,. \tag{18}$$

Therefore, omitting the differential terms (which are only necessary within integrals), the real spectrum is obtained from the following formula

$$\phi(E) = \left(\frac{\rho_0}{\rho}\right)^{1/p} \phi^*\left[\left(\frac{\rho_0}{\rho}\right)^{1/p} E\right]. \tag{19}$$

Compared to the fictitious spectrum – obtained by fitting the Bragg curve assuming bulk LiF – the true spectrum will be slightly higher in intensity, narrower, and shifted toward lower energies.

3. Example

The example presented below serves solely to confirm the validity of Eq. (19). Therefore, the pseudo-experimental scenario of a thin LiF film with a given packing density deposited on a substrate is not considered. This is because such a configuration would introduce complications related to multiple Coulomb scattering and the resulting migration of beam protons from the substrate into the film, thereby distorting the Bragg curve within the film and preventing a clean validation of the equation in question.

For this purpose, consider a hypothetical block of low-density LiF with a density $\rho < \rho_0 = 2.635$ g/cm^3. Specifically, let us assume $\rho = 2.37$ g/cm^3, a value corresponding to a packing density of approximately 89.94%. Using FLUKA (version 4–5.0), the energy deposition profile of a pencil proton beam in this low-density LiF is simulated. The beam energy spectrum chosen for this example follows an exponentially modified Gaussian (EMG) distribution with negative skewness, defined as

$$\phi(E) = \frac{\lambda}{2} \exp\left[-\lambda\left(\mu - E - \sigma^2 \frac{\lambda}{2}\right)\right]\left[1 + \operatorname{erf}\left(\frac{\mu - E - \sigma^2\lambda}{\sqrt{2}\,\sigma}\right)\right]. \tag{20}$$

In this equation, λ, μ, and σ are parameters that determine the shape of the distribution. The following parameter values are set:

$$\lambda = 1.5\ \mathrm{MeV}^{-1}, \quad \mu = 5\ \mathrm{MeV}, \quad \sigma = 0.2\ \mathrm{MeV}. \tag{21}$$

The approach used to process the FLUKA simulation of the energy deposition profile in low-density LiF and to derive the corresponding spectrum follows the method described in [5], with the addition of the transformation presented in Eq. (19). The main details and parameters of the FLUKA simulation are as follows: externally provided EMG energy spectrum – Eqs. (20) and (21) – sampled at 200 points between 0 and 6 MeV; 500,000 virtual protons; low-density (ρ = 2.37 g/cm^3) LiF solid with an entry face of 2×2 cm^2 and a length of 1 cm along the proton propagation direction; FLUKAFIX card configured with Ekin frac = 0.01; USRBIN energy detector positioned at the crystal entry face, with a surface area of 100×100 μm^2 and a depth of 250 μm. The method described in [5], together with the spectral transformation of Eq. (19), has been implemented into a single Matlab [20] program. The results of the best fit are presented in Fig. 1.

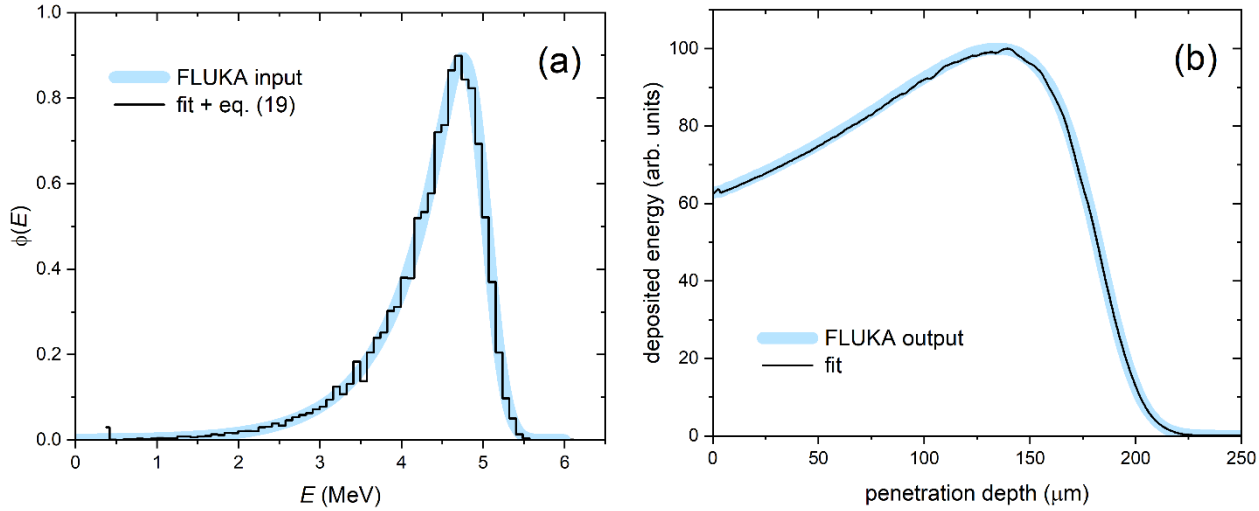

Figure 1. Results related to the proposed example: (a) energy spectrum used as input for FLUKA, along with its fit and the spectral transformation described by Eq. (19); (b) energy deposition profile in low-density LiF (ρ = 2.37 g/cm^3) obtained from the FLUKA simulation, including its fit.

Going into detail, the Matlab program was applied to the FLUKA output by dividing the spectral interval between 0 and 6.5 MeV into 70 bins of equal width. The bootstrap phase, used to estimate the median distributions and their associated uncertainties, consisted of 100 cycles with 20,000 iterations each. The curves labeled 'fit' in Fig. 1 represent these median distributions, including the application of Eq. (19) to derive the real energy spectrum. The parameter used for the spectral transformation was p = 1.71, a value previously estimated – as mentioned in Sec. 2.1 – via allometric fitting of range values in bulk LiF obtained from SRIM [14,15] simulations for energies between 0.5 and 7 MeV. Figure 1(a) shows that the fitted spectrum, after applying the spectral transformation of Eq. (19), accurately reproduces the EMG spectrum used as input for the FLUKA simulation. This confirms the reliability of Eq. (19).

4. Conclusions

In this Technical Report, it has been demonstrated how the energy spectrum of a proton beam can be approximately evaluated by analyzing the luminescent Bragg curve imprinted in a block of LiF with a density lower than that of bulk LiF (e.g., in the case of a thin LiF film). The method employed builds upon the approach previously published for analysis in a LiF crystal [5], followed by a simple variable transformation – Eq. (19) – mediated by the Bragg-Kleeman's law parameter p. The provided example,

based on a spectral EMG distribution used as input in a FLUKA energy deposition simulation, confirms the validity of the proposed approach.

In conclusion, the proposed method enables accurate correction of energy spectra for reduced-density LiF without additional MC simulations. This approach preserves the functional consistency of Bragg-curve analysis and can be in principle generalized to other materials with minor density deviations.

Acknowledgments

I am grateful to my colleague Dr. Massimo Piccinini (ENEA NUC-TECFIS-MNF) for his critical reading of the manuscript. This research has been carried on within the TOP-IMPLART (Oncological Therapy with Protons – Intensity Modulated Proton Linear Accelerator for Radiotherapy) project funded by Regione Lazio, Italy.

References

[1] M. Piccinini, C. Ronsivalle, A. Ampollini, G. Bazzano, L. Picardi, P. Nenzi, E. Trinca, M. Vadrucci, F. Bonfigli, E. Nichelatti, M. A. Vincenti, and R. M. Montereali, *Proton beam spatial distribution and Bragg peak imaging by photoluminescence of color centers in lithium fluoride crystals at the TOP-IMPLART linear accelerator*, Nucl. Instrum. Methods Phys. Res. A **872**, 41–51 (2017).

[2] E. Nichelatti, M. Piccinini, A. Ampollini, L. Picardi, C. Ronsivalle, F. Bonfigli, M. A. Vincenti, and R. M. Montereali, *Bragg-curve imaging of 7 MeV protons in a lithium fluoride crystal by fluorescence microscopy of colour centres*, Europhys. Lett. **120**, 56003 (2017).

[3] M. Piccinini, E. Nichelatti, C. Ronsivalle, A. Ampollini, G. Bazzano, F. Bonfigli, P. Nenzi, V. Surrenti, E. Trinca, M. Vadrucci, M. A. Vincenti, L. Picardi, and R. M. Montereali, *Visible photoluminescence of color centers in LiF crystals for advanced diagnostics of 18 and 27 MeV proton beam*s, Radiat. Meas. **124**, 59–62 (2019).

[4] E. Nichelatti, M. Piccinini, P. Nenzi, L. Picardi, C. Ronsivalle, and R. M. Montereali, *Proton-beam energy diagnostics by color-center photoluminescence imaging in LiF crystals: implementation of multiple Coulomb scattering into an analytical Bragg-curve model*, Nucl. Instrum. Methods Phys. Res. B **547**, 165207 (2024).

[5] E. Nichelatti, M. Piccinini, A. Ampollini, P. Anello, M. D. Astorino, G. Bazzano, E. Cisbani, C. De Angelis, G. Esposito, F. Limosani, P. Nenzi, V. Nigro, C. Ronsivalle, F. Santavenere, V. Surrenti, E. Trinca, M. A. Vincenti, and R. M. Montereali, *Energy spectrum of protons below 10 MeV using color-center radiophotoluminescence in LiF crystals: A Monte Carlo-supported random-optimization estimator*, Nucl. Instrum. Methods Phys. Res. A **1072**, 170218 (2025).

[6] E. Nichelatti, A. Ampollini, M. D. Astorino, G. Bazzano, R. M. Montereali, P. Nenzi, V. Nigro, C. Ronsivalle, V. Surrenti, E. Trinca, M. A. Vincenti, and M. Piccinini, *Energy diagnostics of the TOP-IMPLART linac proton beam via radiophotoluminescence of color centers in lithium fluoride*, Radiat. Meas. **181**, 107369 (2025).

[7] J. C. Spall, *Stochastic Optimization*, in Handbook of Computational Statistics — Concepts and Methods, edited by J. E. Gentle, W. Härdle, and Y. Mori, pages 169–197, Berlin, 2004, Springer.

[8] P. Patnaik, *Handbook of Inorganic Chemicals*, McGraw-Hill, New York, 2002.

[9] FLUKA website: https://fluka.cern.

[10] G. Battistoni, T. Boehlen, F. Cerutti, P. W. Chin, L. S. Esposito, A. Fassò, A. Ferrari, A. Lechner, A. Empl, A. Mairani, A. Mereghetti, P. Garcia Ortega, J. Ranft, S. Roesler, P. R. Sala, V. Vlachoudis, and G. Smirnov, *Overview of the FLUKA code*, Ann. Nucl. Energy **82**, 10–18 (2015).

[11] C. Ahdida, D. Bozzato, D. Calzolari, F. Cerutti, N. Charitonidis, A. Cimmino, A. Coronetti, G. L. D'Alessandro, A. Donadon Servelle, L. S. Esposito, R. Froeschl, R. Garćıa Alía, A. Gerbershagen, S. Gilardoni, D. Horváth, G. Hugo, A. Infantino, V. Kouskoura, A. Lechner, B. Lefebvre, G. Lerner, M. Magistris, A. Manousos, G. Moryc, F. Ogallar Ruiz, F. Pozzi, D. Prelipcean, S. Roesler, R. Rossi, M. Sabaté Gilarte, F. Salvat Pujol, P. Schoofs, V. Stránský, C. Theis, A. Tsinganis, R. Versaci, V. Vlachoudis, A. Waets, and M. Widorski, *New Capabilities of the FLUKA Multi-Purpose Code*, Front. Phys. **9**, 788253 (2022).

[12] V. Vlachoudis, FLAIR: *A Powerful But User Friendly Graphical Interface For FLUKA*, in Proc. Int. Conf. on Mathematics, Computational Methods & Reactor Physics (M&C 2009), Saratoga Springs, New York, 2009.

[13] R. M. Montereali, V. Nigro, M. Piccinini, M. A. Vincenti, A. Ampollini, P. Nenzi, C. Ronsivalle, and E. Nichelatti, *Bragg Curve Detection of Low-Energy Protons by Radiophotoluminescence Imaging in Lithium Fluoride Thin Films*, Sensors **23**, 4779 (2023).

[14] J. F. Ziegler, J. P. Biersack, and M. D. Ziegler, *SRIM – The Stopping and Range of Ions in Matter*, SRIM Co., Chester, Maryland, 2008.
[15] J. F. Ziegler, M. D. Ziegler, and J. P. Biersack, *SRIM – The stopping and range of ions in matter (2010)*, Nucl. Instrum. Methods Phys. Res. B **268**, 1818–1823 (2010).
[16] F. Knoll, *Radiation Detection and Measurement*, John Wiley & Sons, New York, NY, fourth edition, 2010.
[17] E. Nichelatti, C. Ronsivalle, M. Piccinini, L. Picardi, and R. M. Montereali, *An analytical approximation of proton Bragg curves in lithium fluoride for beam energy distribution analysis*, Nucl. Instrum. Methods Phys. Res. B **446**, 29–36 (2019).
[18] T. Bortfeld, *An analytical approximation of the Bragg curve for therapeutic proton beams*, Med. Phys. **24**, 2024–2033 (1997).
[19] B. Gottschalk, *Physics of proton interactions in matter*, in Proton Therapy Physics, edited by H. Paganetti, pages 19–59, Boca Raton, USA, 2011, CRC Press.
[20] The MathWorks, Inc., Matlab, Version 7.10.0 (R2010a), Natick, MA, USA, 2010.

ENEA
Servizio Promozione e Comunicazione
www.enea.it

Stampa: Laboratorio Tecnografico ENEA - Centro Ricerche Frascati

settembre 2025